

1 **Organic aerosol evolution and transport observed at Mt.**
2 **Cimone (2165 m asl), Italy, during the PEGASOS**
3 **campaign**

4

5 **M. Rinaldi¹, S. Gilardoni¹, M. Paglione¹, S. Sandrini¹, S. Fuzzi¹, P. Massoli², P.**
6 **Bonasoni¹, P. Cristofanelli¹, A. Marinoni¹, V. Poluzzi³ and S. Decesari¹.**

7 [1]{National Research Council, Institute of Atmospheric Sciences and Climate, Bologna,
8 Italy}

9 [2]{Aerodyne Research Inc., Billerica, MA, USA}

10 [3]{Centro Tematico Regionale Aree Urbane, Arpa Emilia-Romagna, Bologna, Italy}

11 Correspondence to: M. Rinaldi (m.rinaldi@isac.cnr.it)

12

13 **Abstract**

14 High resolution aerosol mass spectrometer measurements have been performed, for the
15 first time, at the Mt. Cimone Global Atmosphere Watch (GAW) station between June and
16 July 2012, within the EU project PEGASOS and the ARPA–Emilia Romagna project
17 SUPERSITO. Sub-micron aerosol was dominated by organics (63%), with sulphate,
18 ammonium and nitrate contributing for the remaining 20%, 9% and 7%, respectively.
19 Organic aerosol (OA) was in general highly oxygenated, consistent with the remote
20 character of the site; our observations suggest that oxidation and secondary organic aerosol
21 (SOA) formation processes occurred during aerosol transport to high altitudes. All of the
22 aerosol component concentrations as well as the OA elemental ratios showed a clear daily
23 trend, driven by the evolution of the planetary boundary layer (PBL) and by the mountain
24 wind regime. Higher loadings and lower OA oxidation levels were observed during the
25 day, when the site was within the PBL, and therefore affected by relatively fresh aerosol
26 transported from lower altitudes. Conversely, lower loadings and higher OA oxidation
27 levels were observed at night, when the top of Mt. Cimone resided in the free troposphere

1 although affected by the transport of residual layers on several days of the campaign.
2 Analysis of the elemental ratios in a Van Krevelen space shows that OA oxidation follows
3 a slope comprised between -0.5 and -1, consistent with addition of carboxylic groups, with
4 or without fragmentation of the parent molecules. The increase of carboxylic groups during
5 OA ageing is confirmed by the increased contribution of organic fragments containing
6 more than one oxygen atom in the free troposphere night-time mass spectra. Finally,
7 positive matrix factorization was able to deconvolve the contributions of relatively fresh
8 OA (OOAa) originating from the PBL, more aged OA (OOAb) present at high altitudes
9 during periods of atmospheric stagnation, and very aged aerosols (OOAc) transported over
10 long distances in the free troposphere.

11

12 **1 Introduction**

13 Atmospheric aerosols have been intensively studied in the last decades because of their
14 effects on climate, air quality and ecosystems. In many environments, organic aerosol (OA)
15 constitutes a dominant fraction of submicron particles mass (Zhang et al., 2007; Jimenez
16 et al., 2009). OA is made of thousands of individual compounds that can either be emitted
17 directly into the atmosphere (i.e., primary OA or POA) or formed through chemical and
18 physical processes (i.e. secondary OA or SOA). Given the extremely wide range of
19 properties (polarity, vapour pressure, etc.) and number of compounds, typically only 10-
20 20% of the OA mass can be speciated at the molecular level (Seinfeld and Pankow, 2003).

21 OA is a dynamic component, experiencing both atmospheric oxidation and reversible
22 partitioning. This processing (usually referred as ageing) is generally not completely
23 understood and not well represented in models (Heald et al., 2010). In the last decade, on-
24 line instruments like the Aerodyne Research Inc. aerosol mass spectrometer (AMS) (Jayne
25 et al., 2000; Canagaratna et al., 2007) have provided new insights into OA chemical
26 composition and simplified ways of characterizing atmospheric OA ageing. Ng et al.
27 (2010) showed that OA composition tends to become less variable with photochemical
28 ageing, regardless of their source, with the most oxidized spectra resembling that of fulvic
29 acid. Heald et al. (2010) applied the Van Krevelen diagram (H:C vs. O:C space) to the
30 elemental composition of ambient and laboratory OA, observing that bulk OA elemental

1 ratios follow a line characterized by a slope of -1 . This implies that OA ageing involves,
2 on average, the addition of carboxylic acids or equal amounts of hydroxyl and carbonyl
3 functionalities. By contrast, based on a world-wide dataset, Ng et al. (2011) observed a
4 slope of ~ -0.5 for the oxidation of SOA which is characteristic of addition of alcohol,
5 carbonyl and carboxyl functionalities during the ageing process, or of the addition of
6 carboxylic groups accompanied by a C-C bond cleavage (molecular fragmentation).
7 Recently, Holzinger et al. (2013) showed that fragmentation gains importance over
8 functionalization as photochemical age of OA increases, as originally proposed by Kroll et
9 al. (2009). Finally, both ambient observations (Jimenez et al., 2009; Morgan et al., 2010)
10 and laboratory studies (Massoli et al., 2010; Lambe et al., 2011) have pointed out that
11 atmospheric ageing lowers OA volatility and enhances their hygroscopicity, evidencing the
12 importance of atmospheric processing in determining the OA climate relevant properties.

13 In this study, we investigate the atmospheric processing of OA over the Po Valley basin,
14 taking advantage of the unique observatory of Mt. Cimone, part of the Global Atmosphere
15 Watch (GAW) network by the World Meteorological Organization (WMO), a suitable
16 location to study tropospheric background conditions. As many other mountain sites close
17 to anthropogenically-impacted areas, Mt. Cimone provides the opportunity to investigate
18 transport and chemical processing of polluted air masses lifted by convection or by pressure
19 gradients on the mountain slopes (valley breezes) (Marinoni et al., 2008; Gilardoni et al.,
20 2009).

21 The first AMS measurements performed at high altitude mountain stations were reported
22 by Hock et al. (2008) and by Lanz et al. (2008). In particular, the latter study highlighted
23 lower concentrations and higher oxygen content in aerosols collected at the
24 Hohenpeissenberg (Germany) and Jungfrauoch (Switzerland) stations compared to
25 measurements performed simultaneously at low altitude sites. Sun et al. (2009) and Freney
26 et al. (2011) confirmed these findings with measurements performed at Whistler Mountain
27 (Canada), and Puy-de-Dome (France), respectively, and provided useful insights of
28 seasonal effects and air mass origin on the physico-chemical properties of regional aerosol
29 particles measured at elevated sites.

1 The Mt. Cimone GAW/WMO Station is a high altitude research site located in the North
2 Italian Apennines, facing the heavily populated and industrialized Po Valley region. In this
3 study, we present and discuss online sub-micron aerosol chemical composition data
4 collected at Mt. Cimone by a high resolution time of flight aerosol mass spectrometer, HR-
5 ToF-AMS (DeCarlo et al., 2006), during summer 2012, within the EU project PEGASOS
6 and of the Agenzia Regionale per la Prevenzione e l'Ambiente (ARPA) – Emilia Romagna
7 SUPERSITO project. The measurements were used to characterize the summer
8 background aerosol transported into the Po Valley basin area, the vertical transport of
9 anthropogenic aerosol from the lower troposphere (typical of summer circulation), and the
10 regional scale oxidation of OA. Prior to this study, aerosol chemical composition data for
11 Mt. Cimone station were reported by Putaud et al. (2004), Marenco et al. (2006), Carbone
12 et al. (2010) and Carbone et al. (2014) using offline aerosol characterization techniques
13 (i.e., filter samples analysed by ion chromatography and organic carbon analysis). All these
14 papers evidenced the importance of the OA fraction in sub-micron aerosol at the site, both
15 in summer and winter. However, this is the first time that online characterization of
16 atmospheric aerosol, particularly of OA, was performed with high resolution on a mountain
17 site at the centre of the Mediterranean climate hot-spot region.

18

19 **2 Methods**

20 **2.1 Sampling site**

21 Mt. Cimone is the highest peak of the North Italian Apennines. The top of Mt. Cimone
22 ($44^{\circ} 11' N$, $10^{\circ} 42' E$, 2165m a.s.l.) hosts the Italian Climate Observatory “O. Vittori” that
23 is part of the GAW program of the WMO. The station is situated at the southern border of
24 the Po Valley, which is a highly populated and industrialized area, also characterized by
25 intense agricultural activities. Anticyclonic conditions often favour a reduced ventilation
26 within the basin promoting the build-up of lower troposphere aerosols and pollutants.

27 Measurements of atmospheric components carried out at this site are generally considered
28 representative for the South European free troposphere (Bonasoni et al., 2000; Fischer et
29 al., 2003). Nevertheless, due to enhanced vertical mixing occurring during summer months,

1 a daytime influence at Mt. Cimone from the PBL has been documented (Fischer et al.,
2 2003; Cristofanelli et al., 2007). For these reasons, this measurement site can represent a
3 suitable location to investigate the influence of both local and long range transport of
4 polluted air masses on the free troposphere composition (Marinoni et al., 2008).

5 **2.2 Online aerosol chemical characterization**

6 The mass loading and the size-resolved chemical composition of submicron aerosol
7 particles was characterized online by the Aerodyne HR-ToF-AMS. The HR-ToF-AMS
8 provides measurements of the non-refractory sulphate, nitrate, ammonium, chloride, and
9 organic mass in submicron particles (NR-PM₁). During the whole campaign, the HR-ToF-
10 AMS was operating by alternating between “V” and “W” ion path modes every 5 min. The
11 V-mode is characterized by higher sensitivity and lower mass resolution, while the W-
12 mode provides higher mass resolution, but lower sensitivity. The concentrations reported
13 here correspond to the data collected in V-mode. In V-mode, the instrument also acquires
14 information about size distribution of particles, or particle time-of-flight, pToF (Jimenez
15 et al., 2003). The AMS has an effective 50% cut-off for particle sizes below 80 nm and
16 above 600 nm in vacuum aerodynamic diameter (d_{va}) as determined by the transmission
17 characteristics of the standard aerodynamic lens (Liu et al., 2007). Changes in ambient
18 pressure may lead to changes in lens transmission efficiencies (Liu et al., 2007; Bahreini
19 et al., 2008), but such effects are not expected to be significant at the pressure conditions
20 typical of Mt. Cimone (Liu et al., 2007; Sun et al., 2009). However, the particle velocity
21 calibration was adjusted to the altitude (and pressure) conditions of the Mt. Cimone site
22 before starting of the measurements. Ionization efficiency (IE) calibrations were performed
23 before and after the campaign and once per week during the campaign. Filter blank
24 acquisitions during the campaign were performed at least a couple of times per day to
25 evaluate the background and correct the gas phase contribution. All data were analysed
26 using standard ToF-AMS Analysis software SQUIRREL v1.51 and PIKA v1.10 (D.
27 Sueper, available at: [http://cires.colorado.edu/jimenez-group/ToFAMSResources/
28 ToFSoftware/index.html](http://cires.colorado.edu/jimenez-group/ToFAMSResources/ToFSoftware/index.html)) within Igor Pro 6.2.1 (WaveMetrics, Lake Oswego, OR).
29 Positive matrix factorization (PMF) analyses on the HR-ToF-AMS data were performed
30 using the PMF2.exe algorithm (v.4.2) in robust mode (Paatero and Tapper, 1994). The

1 PMF inputs (mass spectral and error matrices of the OA component) were prepared
2 according to Zhang et al. (2011). The PMF solutions were then evaluated with an Igor Pro-
3 based PMF evaluation tool (PET, v. 2.04) following the method described in Ulbrich et al.
4 (2009) and Zhang et al. (2011). The HR-ToF-AMS collection efficiency (CE) was
5 calculated according to Middlebrook et al. (2012) and evaluated against parallel offline
6 measurements (Fig. S1). The average CE for the campaign was 0.52 ± 0.06 . The propagated,
7 overall uncertainty for the total AMS mass concentration is 20–35% (2σ) according to
8 Middlebrook et al. (2012). The aerosol was sampled via a total suspended particle (TSP)
9 aerosol inlet, which is built according to the EUSAAR/ACTRIS protocol to improve the
10 collection performances at high altitude. The aerosol was dried to about 40% by means of
11 a Nafion drier before sampling with the HR-ToF-AMS.

12

13 **2.3 Additional measurements**

14 Ancillary measurements at Mt. Cimone conducted during the campaign included
15 meteorological parameters and other trace gases (CO , O_3 , NO_x). Trace gas measurements
16 were carried out by using a common sampling system designed for reactive gas sampling,
17 characterized by an intake line located 2 m above the roof and 7 m above the ground and
18 consisting of a glass tube through which the sampled air is passed at a high flow rate (larger
19 than 20 L s^{-1}). Sample air was supplied to the various analysers via a Teflon manifold pipe
20 (about 1 m long) connected to the glass tube. A particle filter (changed regularly every 15-
21 30 days) prevented dust, rain drops and other unwanted material from entering the inlet.

22 Surface ozone (O_3) was continuously measured (1-minute time resolution) by a UV-
23 absorption analyser Dasibi 1108 W/GEN (Cristofanelli et al., 2015). Carbon dioxide (CO)
24 was measured by a NDIR analyser Thermo Tei 49C. Following Henne et al. (2008), the
25 system and sampling procedures have been modified to carry out observations in remote
26 conditions usually characterized by low mixing ratios. During the PEGASOS campaign,
27 NO_x measurements were carried out by a chemiluminescence analyser (Thermo 42C).
28 This instrument is equipped with a molybdenum converter to determine NO_x , which
29 according to Steinbacher et al (2007), can overestimate the NO_2 up to ~50% due to the

1 interference of oxidized nitrogen compounds (NO_x) such as peroxyacetyl-nitrate and nitric
2 acid.

3 The measurement of the aerosol absorption coefficient was obtained by a Multi-Angle
4 Absorption Photometer (MAAP 5012, Thermo Electron Corporation), which measures the
5 transmission and the back scattering of a light beam incident on a fiber filter where aerosol
6 particles are deposited by the sampling flow. The equivalent black carbon (eqBC)
7 concentration has been obtained by using a mass absorption efficiency of $6.5 \text{ m}^2 \text{ g}^{-1}$ as
8 recommended by Petzold et al. (2002)

9 PM_{10} offline aerosol samples were collected on quartz filters as described by Carbone et al.
10 (2014) with a 12 h sampling resolution. Chemical analysis of main inorganic species was
11 performed via ion chromatography and carbon elemental analysis (Carbone et al., 2014).

12

13 **3 Results**

14 **3.1 Online aerosol chemical characterization at Mt. Cimone**

15 Figure 1 shows the time trend of the major non-refractory components of submicron
16 aerosol (NR-PM_{10}) measured at Mt. Cimone during the campaign, together with the time
17 dependent relative mass contribution of the same aerosol components. NR-PM_{10} was clearly
18 dominated by OA through the whole campaign: OA average atmospheric concentration
19 and standard deviation were $2.8 \pm 2.4 \mu\text{g m}^{-3}$, for an average mass contribution of 63%.
20 Sulphate was the second most abundant species with a concentration of $0.92 \pm 0.60 \mu\text{g m}^{-3}$
21 (20%), followed by ammonium ($0.41 \pm 0.33 \mu\text{g m}^{-3}$, 9%) and nitrate ($0.33 \pm 0.46 \mu\text{g m}^{-3}$,
22 7%). Chlorine was usually below the detection limit (80% of the data points) and
23 contributed less than 1 % to the NR-PM_{10} (and was therefore excluded from Figure 1b). For
24 comparison, sub-micrometre aerosol chemical characterization measurements performed
25 in spring and summer at high (Jungfraujoch) and rural (Hohenpeissenberg) sites in Europe
26 (Hock et al., 2008; Lanz et al., 2010) report organics ranging from 43% to 50 %, sulphate
27 ranging from 19% to 26 %, ammonium contributing between 13% and 11% and nitrate
28 ranging from 18% to 19% (see Table 1 for a summary of AMS measurements performed
29 at background measurements sites).

1 The measured ammonium concentrations were in equivalent concentrations to the sum of
2 sulphate, nitrate and chloride, with a slope of 0.99 and a linear correlation coefficient (R)
3 of 0.99. This means that aerosol particles measured at Mt. Cimone were neutralized. The
4 average NR-PM₁ mass during the campaign was $4.5 \pm 3.4 \mu\text{g m}^{-3}$, in fairly good agreement
5 with PM₁ measurements previously performed at the site in the same season, even though
6 with different measurement techniques (Marenco et al., (2006); Carbone et al.(2010);
7 Carbone et al. (2014)). The lowest aerosol mass concentrations were observed during the
8 first days of the campaign up to June 15, when Northern Italy was influenced by a low-
9 pressure system, bringing unstable conditions. Conversely, the highest concentrations were
10 recorded between June 17 and 20 under high pressure conditions characterized by anti-
11 cyclonic circulation (Decesari et al., in preparation), which is known to favour the
12 stagnation of local pollutants produced within the Po Valley basin (See Fig. S2 for further
13 details).

14 The results of the elemental analysis (EA) of the organic fraction are presented in Figure 2
15 as time trends of the H:C, O:C and OM:OC ratios. Average H:C, O:C and OM:OC ratio
16 measured during the campaign are 1.45 ± 0.11 , 0.71 ± 0.08 and 2.08 ± 0.10 , respectively,
17 corresponding to an average oxidation state ($\text{OS}_c = 2 \cdot \text{O:C} - \text{H:C}$; Kroll et al. (2011)) of -
18 0.02 ± 0.23 . These ratios are indicative of a highly oxygenated organic aerosol, in agreement
19 with previous AMS measurements at mountain sites (Freney et al., 2011; Lanz et al., 2010).
20 The values have been calculated using the improved-Ambient (I-A) EA method to derive
21 OA elemental ratios from AMS spectra (Canagaratna et al., 2015).

22 The corresponding EA values calculated using the Aiken-Ambient (A-A) method (Aiken
23 et al., 2008), are 1.32 ± 0.08 , 0.58 ± 0.07 and 1.89 ± 0.09 , respectively, corresponding to an
24 average oxidation state ($\text{OS}_c = 2 \cdot \text{O:C} - \text{H:C}$) of -0.16 ± 0.22 . The elemental ratios calculated
25 with the A-A method are reported here just for the purpose of a more direct comparison
26 with papers published before the introduction of the new I-A method (2015). Anyway,
27 through all the paper and in the plots, the more accurate I-A elemental ratios will be
28 reported. Saarikoski et al. (2012) present results of HR-ToF-AMS measurements in the Po
29 Valley at the site of San Pietro Capofiume (SPC) during April 2008, showing an average
30 H:C ratio slightly higher (1.49) and an average O:C ratio slightly lower (0.47) than those
31 observed at Mt. Cimone, for a resulting average OM:OC ratio of 1.77. Similarly, OM:OC

1 higher than 1.7 were observed in the outflow plume over Mexico city and at the mountain
2 site of Altzomoni, above the Mexico city plateau (Gilardoni et al., 2009). The OM:OC ratio
3 observed at SPC in Fall 2011 was 1.6 (Gilardoni et al., 2014). The lower oxidation of the
4 OA collected at SPC during spring and fall with respect to the present measurements can
5 be due to (a) the different season or (b) to oxidation processes involving OA during
6 transport from low altitude sites up to Mt. Cimone. This last aspect will be investigated in
7 Section 3.3.

8 **3.2 Analysis of the diurnal cycles**

9 The atmospheric concentrations of the major NR-PM₁ components present a clear diurnal
10 cycle with maxima at the early afternoon and minima during the night (Figure 3). The
11 concentration daily trend of the NR-PM₁ components is the result of the PBL dynamics
12 and valley breezes, as during the night the site is well above the shallow nocturnal layer
13 forming over the Po Valley plain and disconnected from the aerosol sources located at the
14 low altitudes. However, Marinoni et al. (2008) showed that in summer, during the night-
15 time, Mt. Cimone station may be affected by polluted air masses present in the residual
16 layer above the Po Valley. Conversely, during the day, with the increase of the PBL height,
17 the site is affected by convective transport from lower altitudes (Schuepbach et al., 2001;
18 Fischer et al., 2003; Freney et al., 2011) and it is directly connected to the pollution sources
19 located in the valley, thus experiencing high aerosol concentrations. During PEGASOS,
20 the time trend of OA (the major contributor to NR-PM₁) correlates with that of specific
21 humidity (SH), which can be used as a tracer of PBL air at high altitudes (Henne et al.,
22 2005) (Figure S3). This good correlation strongly supports the hypothesis that the aerosol
23 transport triggered by the PBL dynamics is the main factor regulating the NR-PM₁
24 concentrations at Mt. Cimone during the measurement period.

25 To further investigate the importance of vertical transport from the PBL to the top of Mt.
26 Cimone during the day, we calculated the daily relative increase (RI) in SH, following the
27 approach introduced by Prevôt et al. (2000) and Henne et al. (2005) for two different sites
28 in the Alps and already applied for Mt. Cimone station by Carbone et al. (2014).

29

$$1 \quad RI = \frac{SH_{aft}(CMN) - SH_{mor}(CMN)}{SH_{aft}(SPC) - SH_{mor}(CMN)} \quad (1)$$

2

3 In Equation 1, $SH_{aft}(CMN)$ is the average specific humidity measured in the afternoon at
4 Mt. Cimone (12:00 to 18:00 LT), $SH_{mor}(CMN)$ is the average specific humidity measured
5 during the night at Mt. Cimone (22:00 to 05:00 LT) and $SH_{aft}(SPC)$ is the average specific
6 humidity measured in the afternoon (12:00 to 18:00 LT) at the rural background station of
7 San Pietro Capofiume (SPC), located in the Po Valley 90 km north-east of Mt. Cimone at
8 11 m a.s.l. and considered representative of PBL conditions within the Po Valley basin. A
9 RI of 1 corresponds to a complete replacement of the high altitude air by boundary layer
10 air, while no vertical motion yields zero relative increase. RI was calculated for each day
11 of the campaign and the average value was 0.8 ± 0.3 , confirming the high influence of
12 vertical convection during the day at the station in summer.

13 Similarly to the NR- PM_{10} components, OA elemental ratios exhibit diurnal variations (Fig
14 4). The O:C and OM:OC ratios have lower values in the afternoon and maxima at night,
15 with a minimum O:C hourly average of 0.67 ± 0.10 observed between 14:00 and 15:00, and
16 maximum of 0.75 ± 0.08 between 00:00 and 01:00. An opposite trend is observed for the
17 H:C ratio, with a maximum hourly average of 1.55 ± 0.10 between 14:00 and 15:00, and a
18 minimum of 1.38 ± 0.10 between 00:00 and 01:00. The daily trend of the O:C and OM:OC
19 ratio are almost coincident (correlation coefficient 0.999) confirming the results of Pang et
20 al. (2006) showing that the OM:OC ratio is mainly regulated by the O:C ratio.

21 These trends highlight the different age of the aerosols measured at the sampling location
22 in different moments of the day, as a consequence of the PBL dynamics. In fact, the O:C
23 ratio of OA tends to increase and the H:C ratio decreases as a function of its atmospheric
24 residence time, because of the oxidation of reduced species emitted by traffic and
25 combustion and of SOA formation (Aiken et al., 2008; DeCarlo et al., 2008; Heald et al.,
26 2010; Chhabra et al., 2011; Ng et al., 2011; Sun et al., 2011b; Sun et al., 2011a). Particles
27 sampled at Mt. Cimone during the day are representative of an early stage of aerosol
28 atmospheric oxidation, resulting from SOA formed at lower altitudes in the Po Valley and
29 transported upward by turbulence and by thermal winds, typically in few hours. By

1 contrast, at night the aerosol sampled at Mt. Cimone is more processed, as the atmospheric
2 layers affecting the site at night contain aerosols with an age from several hours (residual
3 layers) to days (from long-range transport). This is confirmed by the CO/NO_x ratio, often
4 used in the literature as a tracer for air mass photochemical age (Morgan et al., 2010; Freney
5 et al., 2011). CO/NO_x at Mt. Cimone is 159±65 (average ± standard deviation) during the
6 daytime and 287±168 at night, which is a value representative of aged regional emissions.
7 The CO/NO_x ratio is presented in detail in Figure S4, showing clearly that during the night-
8 time the CO/NO_x ratio is systematically higher than during daytime. For these reasons, Mt.
9 Cimone is an ideal site to investigate the processing of organic aerosol over the Po Valley
10 basin. Moreover, according to Marinoni et al. (2008), the footprint of aerosol particles
11 found in the residual layers at night comprises a great part of central Europe, which is the
12 region where the full oxidation of organic aerosols that we observe at Mt. Cimone takes
13 place.

14 **3.3 Investigation of regional scale organic aerosol ageing**

15 To investigate the oxidation of OA, data collected at Mt. Cimone during the campaign have
16 been divided based on the position of the station relative to the PBL height, using SH as a
17 tracer of the PBL evolution. Figure S5 shows the average daily evolution of the SH at Mt.
18 Cimone during the campaign that mimics the PBL evolution during the day: the afternoon
19 maximum indicates that the site is within the PBL, under the influence of moist air coming
20 from lower altitudes, while the night minimum indicates that Mt. Cimone station is above
21 the PBL. Following Figure S5, HR-ToF-AMS measurements collected between 12:00 and
22 18:00 have been considered as PBL samples, those collected between 22:00 and 05:00 have
23 been defined as free troposphere (FT) samples, while all the samples excluded from the
24 previous two groups have been considered as transition samples (TR). As expected, PBL
25 samples were less oxidized (H:C = 1.54±0.06, O:C = 0.69±0.05, OM:OC = 2.05±0.10)
26 than FT samples (H:C = 1.41±0.09, O:C = 0.74±0.07, OM:OC = 2.12±0.10), with TR
27 samples characterized by intermediate values (H:C = 1.45±0.09, O:C = 0.72±0.07, OM:OC
28 = 2.08±0.09), consistent with the average elemental ratios discussed in the Section 3.1. The
29 differences between the average elemental ratios of PBL, TR and FT are statistically
30 significant according to the t-test (p<0.01). The large standard deviations associated to the

1 mean values are due to day-by-day variations, as showed by Figure S6. Figure S6 also
2 shows that, independently on the day-by-day variations, O:C is systematically higher, and
3 H:C systematically lower, in the FT compared to the PBL air masses, while the TR air
4 masses have intermediate values.

5 Figures 5 shows the whole campaign data points in a Van Krevelen diagram (Van
6 Krevelen, 1950), together with the average H:C and O:C ratios of PBL, TR and FT samples.
7 The data are lumped within the region delimited by O:C between 0.5 and 1 and H:C
8 between 1.1 and 1.5. The plot illustrates the process of OA atmospheric oxidation in the
9 investigated area characterized by a slope comprised between -0.5 and -1. According to
10 Heald et al. (2010) and Ng et al. (2011), such an intermediate slope can result from a
11 combination of reactions adding carboxylic acids to the OA, occurring both with and
12 without fragmentation of the parent molecules (expected slopes = -0.5 and -1, respectively).
13 Kroll et al. (2011) reported that fragmentation becomes increasingly important for already
14 oxidized material undergoing further processing. This can explain the results at Mt.
15 Cimone, where OA does not resemble recently formed secondary material, in analogy with
16 Ng et al. (2011). An alternative explanation for a slope tending to -0.5 is given by
17 equivalent amounts of addition of carboxylic groups and of hydroxyls or peroxides (Ng et
18 al., 2011).

19 The addition of carboxylic functionalities during the OA ageing process is confirmed by
20 the analysis of the high resolution mass fragments, showing that, from PBL to FT samples,
21 the average contribution of $C_xH_yO_{z>1}$, attributed to the fragmentation of carboxylic
22 structures (Aiken et al., 2007; Takegawa et al., 2007; Duplissy et al., 2011), increases from
23 35% to 43%, while both C_xH_y and C_xH_yO fragments decrease (Figure 6). The mean
24 elemental compositions calculated for PBL, TR and FT samples fall at distinct positions
25 along the line of average ageing in the Van Krevelen space (Figure 5), suggesting that the
26 observed oxidation of OA is dictated by the different age of the aerosols reaching the
27 station at different times of the day, as also evidenced by Figure S6.

28 Finally, Figure 7 shows the time-of-flight particle size distributions (pToF) of the main
29 NR-PM₁ components as measured by the HR-ToF-AMS observed during the three regimes
30 (PBL, TR and RL). For each species, there is no appreciable size distribution difference

1 between the three sample sub-sets (PBL, TR and FT). However, the organics pToF peaks
2 at a slightly lower d_{va} (293 nm) compared to sulphate, ammonium and nitrate (which peak
3 between 330 and 340 nm d_{va}), as determined by a lognormal fit of the size distributions.
4 This result indicates that the organic and inorganic components in all the sampled air
5 masses are not entirely internally mixed. Furthermore, organics pToF shows a tail towards
6 smaller particles sizes reaching 90 nm, and appreciable amount of mass below 200 nm d_{va} ,
7 which is consistent with previous observations of organics pToF typically having lower d_{va}
8 than e.g., SO_4 , due to different sources and formation processes. It is possible that a fraction
9 of the organics observed at $d_{va} < 200$ nm arises from the growth of smaller particles (fresh
10 emission typically peak at d_{va} of 80-100 nm). via condensation processes during transport
11 to high altitude.

12 **3.4 OA source apportionment by PMF**

13 In order to further characterize the OA collected at Mt. Cimone, PMF was applied to the
14 high-resolution OA mass spectra. We screened various solutions with a number of factors
15 from two to ten. A 4-factor solution with rotational forcing parameter $f_{peak} = 0$ (Q/Q_{exp}
16 $= 2.3$) was chosen, yielding four different types of OOA, two of which were recombined
17 into one factor, because of coincident time series and profiles (Fig. S6). The OA
18 components from the PMF analysis were identified by their mass spectra, elemental
19 composition (Fig. 8) and diurnal cycles (Fig. 9), as well as by correlations of their time
20 series with tracers (Tab. 2). A detailed summary of key diagnostic plots of the PMF results
21 and a discussion of the factor solution choices can be found in the supporting information
22 (SI).

23 The three resulting factors are all of the oxygenated organic aerosol (OOA) type and have
24 been defined as OOAA, OOAB and OOAC. No "standard" hydrocarbon like (HOA) factor
25 (i.e., with m/z 43 \gg m/z 44 and with a significant amount of hydrocarbon-like ions, C_xH_y)
26 could be extracted by PMF, similarly to other AMS datasets collected at background sites
27 (Hildebrandt et al., 2010; Freney et al., 2011), indicating almost no direct influence of
28 freshly emitted primary aerosols to the observed OA load. This result is consistent with the
29 highly oxidized character of the OA, as described previously. Even though m/z 44 (CO_2^+)
30 dominates the mass spectra of all the three factors, the OOAA factor has a slightly higher

1 amount of C_xH_y ions at m/z 27 ($C_2H_3^+$), 39 ($C_3H_3^+$), 41 ($C_3H_5^+$) compared to the other
2 factors.

3 The elemental composition (H:C, O:C) and the OM:OC ratio are also reported in Fig. 8.
4 OOAc is the most oxidized factor, with an OM:OC ratio of 2.48 versus 2.03 and 2.13 of
5 OOAA and OOAB, respectively. Consequently, it has higher O:C (1.02) and lower H:C
6 (1.07) ratio than OOAA (0.67; 1.51) and OOAB (0.75; 1.44). OOAA average concentration
7 was $1.5 \pm 1.7 \mu\text{g m}^{-3}$ during the campaign, which accounts for 55% of the OA. OOAB
8 presented higher concentrations during the period 17-23 June ($2.1 \pm 1.5 \mu\text{g m}^{-3}$) and low
9 concentrations during the rest of the campaign ($0.27 \pm 0.29 \mu\text{g m}^{-3}$), for an average
10 concentration of $0.67 \pm 1.1 \mu\text{g m}^{-3}$ and a contribution of 25%. The concentration of OOAc
11 was $0.54 \pm 0.40 \mu\text{g m}^{-3}$ contributing on average 20% to the OA.

12 When looking at the diurnal profiles of the three factors (Fig. 9), we see clear diurnal cycles
13 for OOAA and OOAc (but with opposite trends, having OOAA a maximum at 16:00, and
14 OOAc having a minimum at 14:00) and a less pronounced diurnal profile for OOAB
15 (slightly higher concentration around 12:00-14:00 than during the rest of the day). The fact
16 that OOAA concentration is much higher during the day than at night indicates that this
17 factor derives from sources located within the PBL and is transported at Mt. Cimone by
18 convection and by thermal winds in daytime, as discussed above. Conversely, the trend for
19 OOAc with lower concentrations during the day points to a transport from the free
20 troposphere, or anyway from above the PBL.

21 The Pearson correlation coefficients (R) between the three PMF factors and several
22 external gas-phase and particle tracers are reported in Table 2. OOAA correlates best with
23 CO, NO_x and BC (0.71, 0.70 and 0.54 respectively), which are attributable to
24 anthropogenic sources located within the PBL, confirming our interpretation of the OOAA
25 source location. OOAB shows lower correlation than OOAA against all the tracers, with
26 higher R values associated with the above enlisted PBL tracers (CO, NO_x and BC),
27 suggesting that this factor too was contributed by PBL sources. Interestingly, OOAB
28 presents the highest correlation with sulphate, which suggests a regional character for this
29 OOA component. The highest correlation for OOAc is with O_3 , with a very small
30 correlation with all the PBL tracers. The high correlation of OOAc with O_3 is mainly driven

1 by the coincident daily trends (Figure S11), showing higher concentration at night, a typical
2 feature of O₃ at high-altitude sites (Fischer et al., 2003; Cristofanelli et al., 2007). In fact,
3 during summer, air-masses richer in photochemically produced O₃ are vented to Mt.
4 Cimone in the afternoon, leading to an increase of O₃ until evening, when O₃ observations
5 start to be more representative of the free troposphere.

6 The spectral and elemental features of the three OOA factors are in the range of others
7 reported in the literature (Mohr et al., 2012; Holzinger et al., 2013; Sun et al., 2011a).
8 Similar OOA spectra have also been described by Saarikoski et al. (2012) for the Po Valley
9 site of San Pietro Capofiume. Correlation analysis with reference high-resolution spectra
10 (Table 3) suggests that all the OOA components identified can be classified as LV-OOA
11 (low volatile-OOA). However, OOAA and OOAB present qualitatively similar spectral
12 features to the SV-OOA (semi volatile-OOA) reported by Freney et al. (2011), for a similar
13 high altitude station, and by Hayes et al. (2013), for photochemically aged aerosol. The f₄₄
14 (contribution of organic mass fragments with m/z 44) of OOAA and OOAB is 0.13 and
15 0.14, respectively, which is across the SV-OOA/LV-OOA region proposed by Cubison et
16 al. (2011). Therefore, we believe that OOAA and OOAB can be considered either as highly
17 oxidized SV-OOA or LV-OOA with a low oxidation level.

18 In summary, OOAA is clearly attributed to sources or formation processes located within
19 the PBL that reach the station when vertical transport (PBL convection and valley/upslope
20 breeze) is maximized. OOAA is the less oxidized factor retrieved by PMF and likely
21 represents a moderately aged local OA. OOAB has a less defined diurnal cycle (still with
22 maximum during daytime) and a slightly higher O:C ratio than OOAA. The period of OOAB
23 maximum contribution coincides with meteorological conditions characterized by reduced
24 horizontal air motion and dominated by breeze regimes (17-23 June, when an anticyclonic
25 high pressure system was present over northern Italy). These conditions favour the
26 accumulation of pollutants within the PBL and in the residual layers above, because of
27 reduced air circulation. Collaud Coen et al. (2011) demonstrated that under such
28 meteorological conditions, air masses from residual layers continue to influence the
29 Jungfraujoch high altitude station also during the night, leading to higher minima in the
30 diurnal aerosol concentration than in other conditions. We postulate that the same happens
31 at Mt. Cimone. The entire region influenced by the high pressure system extends beyond

1 the Po Valley basin, comprising the great Alpine region. Over the Alps, orographic lifting
2 of PBL air is responsible for the formation of residual layers at very high altitudes (the
3 Jungfrauoch is at 3571 m a.s.l.) which can then travel on the top of the PBL over the
4 surrounding basins (like the Po Valley). We therefore hypothesize that factor OOAb is a
5 regional component of NR-PM₁, associated with the accumulation and ageing of OA in
6 residual layers when wind speeds are small throughout the lower troposphere during period
7 of enhanced high pressure conditions. This is also supported by the good correlation
8 between OOAb and regional sulphate.

9 Finally, OOAc is the product of prolonged atmospheric processing of OA, occurring
10 mainly in the free troposphere, and can be considered as representative of the background
11 FT OA on a spatial scale that comprises all western European areas upwind of Mt. Cimone.
12 These conclusions are confirmed by the plots in Figure 10, showing CO/NO_x vs. SH colour
13 coded by the contribution of each factor. Clearly, OOAc is associated with air masses
14 characterized by reduced photochemical age (low CO/NO_x) and strongly influenced by the
15 PBL (high SH), while OOAc contributes more in air masses characterized by high
16 photochemical age (high CO/NO_x) and less influenced by the PBL (low SH). OOAb
17 presents intermediate characteristics (mid to low CO/NO_x and intermediate SH), consistent
18 with the hypothesis that OOAb is representative of OA of intermediate age that is
19 accumulated in the residual layers during the period of high pressure, due to the stagnant
20 atmospheric conditions.

21

22 **4 Conclusions**

23 The chemical composition of non-refractory sub-micrometric particles was measured for
24 the first time by a HR-ToF-AMS at the Mt. Cimone GAW/WMO high altitude station.
25 Sub-micrometric aerosol was dominated by the organic fraction (on average 63%), with
26 ammonium sulphate as second contributor, for an average NR-PM₁ mass of $4.5 \pm 3.4 \mu\text{g m}^{-3}$.
27 Elemental analysis of the high resolution AMS data showed highly oxygenated OA (the
28 campaign-average H:C, O:C and OM:OC were 1.45 ± 0.11 , 0.71 ± 0.08 and 2.08 ± 0.10 ,
29 respectively), suggesting that strong oxidation and SOA formation processes occur during
30 aerosol transport to high altitudes. Different stages of OA processing could be identified

1 when comparing the OA composition during daytime, when the station was affected by the
2 upward transport of PBL air, and the night-time, when the site was in the free troposphere
3 (FT).

4 Analysis of the OA elemental ratios in a Van Krevelen space showed that OA oxidation
5 followed a slope comprised between -0.5 and -1, consistent with the addition of carboxylic
6 groups to alkyl structures, occurring both with and without fragmentation of the reagent
7 molecules. The increase of carboxylic groups during OA processing and ageing is
8 confirmed by the increased contribution of $C_xH_yO_{z>1}$ fragments during night-time
9 measurements.

10 Quantitative information on the contributions of more and less aged OA components were
11 achieved by analysing the high resolution AMS data by positive matrix factorization
12 (PMF). OOAA (55%), the least oxidized OOA factor, was related to sources or formation
13 processes located within the PBL, reaching the station mainly during day-time, when
14 vertical transport is maximized. OOAB (25%) was attributed to the accumulation and
15 ageing of OA in the PBL and in the residual layers above the PBL, due to stagnation over
16 the great Alpine region. Finally, OOAC (20%) was interpreted as the product of prolonged
17 atmospheric processing of OA occurring mainly above the PBL, and can be considered as
18 representative of background free tropospheric OA at a continental scale.

19 This work highlights the important contribution of organic aerosols to the composition of
20 submicron particles at remote mountain sites. We found that 63% of the NR-PM₁ mass that
21 constitutes the background aerosol levels for the Po Valley in the summer is accounted for
22 by highly oxygenated organic matter. No important contribution from primary combustion
23 organic particles (HOA) was measured, indicating that these compounds were likely lost
24 during transport either by evaporation or chemical processing. Most importantly, in spite
25 of the vicinity of strongly emitting pollution sources in the Po Valley, only 55% of the
26 organic matter measured at Mt. Cimone in the summer could be attributed to sources within
27 the PBL, while the remaining fraction (45%) is accounted for by remote upwind sources.
28 This study confirms the importance of regional scale physical and chemical processes and
29 of transboundary transport in determining the background aerosol composition at rural
30 European sites.

1

2 **Acknowledgements**

3 This work was supported by the projects PEGASOS and BACCHUS funded by the
4 European Commission under the Framework Programme 7 (FP7-ENV-2010-265148 and
5 FP7-603445) and by the project SUPERSITO funded by Regione Emilia Romagna (DRG
6 no. 428/10). Continuous atmospheric observation programmes at Mt. Cimone are
7 supported by the Project of National Interest NextData, funded by Italian Ministry for
8 Education, University and Research and by EU-ACTRIS project.

9 Maria Cristina Facchini is acknowledged for the helpful suggestions. Leone Tarozzi,
10 Francesca Pollini and Francescopiero Calzolari are acknowledged for the technical support.

11

1 **References**

- 2 Aiken, A. C., DeCarlo, P. F., and Jimenez, J. L.: Elemental analysis of organic species with
3 electron ionization high-resolution mass spectrometry, *Analytical Chemistry*, 79, 8350-
4 8358, 10.1021/ac071150w, 2007.
- 5 Aiken, A. C., Decarlo, P. F., Kroll, J. H., Worsnop, D. R., Huffman, J. A., Docherty, K. S.,
6 Ulbrich, I. M., Mohr, C., Kimmel, J. R., Sueper, D., Sun, Y., Zhang, Q., Trimborn, A.,
7 Northway, M., Ziemann, P. J., Canagaratna, M. R., Onasch, T. B., Alfarra, M. R., Prevot,
8 A. S. H., Dommen, J., Duplissy, J., Metzger, A., Baltensperger, U., and Jimenez, J. L.: O/C
9 and OM/OC ratios of primary, secondary, and ambient organic aerosols with high-
10 resolution time-of-flight aerosol mass spectrometry, *Environmental Science &*
11 *Technology*, 42, 4478-4485, 10.1021/es703009q, 2008.
- 12 Bahreini, R., Dunlea, E. J., Matthew, B. M., Simons, C., Docherty, K. S., DeCarlo, P. F.,
13 Jimenez, J. L., Brock, C. A., and Middlebrook, A. M.: Design and operation of a pressure-
14 controlled inlet for airborne sampling with an aerodynamic aerosol lens, *Aerosol Science*
15 *and Technology*, 42, 465-471, 10.1080/02786820802178514, 2008.
- 16 Bonasoni, P., Evangelisti, F., Bonafe, U., Ravegnani, F., Calzolari, F., Stohl, A., Tositti,
17 L., Tubertini, O., and Colombo, T.: Stratospheric ozone intrusion episodes recorded at Mt.
18 Cimone during the VOTALP project: case studies, *Atmospheric Environment*, 34, 1355-
19 1365, 10.1016/s1352-2310(99)00280-0, 2000.
- 20 Canagaratna, M., Jayne, J., Jimenez, J., Allan, J., Alfarra, M., Zhang, Q., Onasch, T.,
21 Drewnick, F., Coe, H., Middlebrook, A., Delia, A., Williams, L., Trimborn, A., Northway,
22 M., DeCarlo, P., Kolb, C., Davidovits, P., and Worsnop, D.: Chemical and microphysical
23 characterization of ambient aerosols with the aerodyne aerosol mass spectrometer, *Mass*
24 *Spectrometry Reviews*, 26, 185-222, 10.1002/mas.20115, 2007.
- 25 Canagaratna, M. R., Jimenez, J. L., Kroll, J. H., Chen, Q., Kessler, S. H., Massoli, P., Ruiz,
26 L. H., Fortner, E., Williams, L. R., Wilson, K. R., Surratt, J. D., Donahue, N. M., Jayne, J.
27 T., and Worsnop, D. R.: Elemental ratio measurements of organic compounds using aerosol
28 mass spectrometry: characterization, improved calibration, and implications, *Atmospheric*
29 *Chemistry and Physics*, 15, 253-272, 10.5194/acp-15-253-2015, 2015.

1 Carbone, C., Decesari, S., Mircea, M., Giulianelli, L., Finessi, E., Rinaldi, M., Fuzzi, S.,
2 Marinoni, A., Duchi, R., Perrino, C., Sargolini, T., Varde, M., Sprovieri, F., Gobbi, G. P.,
3 Angelini, F., and Facchini, M. C.: Size-resolved aerosol chemical composition over the
4 Italian Peninsula during typical summer and winter conditions, *Atmospheric Environment*,
5 44, 5269-5278, 10.1016/j.atmosenv.2010.08.008, 2010.

6 Carbone, C., Decesari, S., Paglione, M., Giulianelli, L., Rinaldi, M., Marinoni, A.,
7 Cristofanelli, P., Didiodato, A., Bonasoni, P., Fuzzi, S., and Facchini, M. C.: 3-year
8 chemical composition of free tropospheric PM₁ at the Mt. Cimone GAW global station -
9 South Europe - 2165 m a.s.l, *Atmospheric Environment*, 87, 218-227,
10 10.1016/j.atmosenv.2014.01.048, 2014.

11 Chhabra, P. S., Ng, N. L., Canagaratna, M. R., Corrigan, A. L., Russell, L. M., Worsnop,
12 D. R., Flagan, R. C., and Seinfeld, J. H.: Elemental composition and oxidation of chamber
13 organic aerosol, *Atmospheric Chemistry and Physics*, 11, 8827-8845, 10.5194/acp-11-
14 8827-2011, 2011.

15 Collaud Coen, M., Weingartner, E., Furger, M., Nyeki, S., Prevot, A. S. H., Steinbacher,
16 M., and Baltensperger, U.: Aerosol climatology and planetary boundary influence at the
17 Jungfraujoch analyzed by synoptic weather types, *Atmospheric Chemistry and Physics*, 11,
18 5931-5944, 10.5194/acp-11-5931-2011, 2011.

19 Cristofanelli, P., Bonasoni, P., Carboni, G., Calzolari, F., Casarola, L., Sajani, S. Z., and
20 Santaguida, R.: Anomalous high ozone concentrations recorded at a high mountain station
21 in Italy in summer 2003, *Atmospheric Environment*, 41, 1383-1394,
22 10.1016/j.atmosenv.2006.10.017, 2007.

23 Cristofanelli, P., Scheel, H. E., Steinbacher, M., Saliba, M., Azzopardi, F., Ellul, R.,
24 Froehlich, M., Tositti, L., Brattich, E., Maione, M., Calzolari, F., Duchi, R., Landi, T. C.,
25 Marinoni, A., and Bonasoni, P.: Long-term surface ozone variability at Mt. Cimone
26 WMO/GAW global station (2165 m a.s.l., Italy), *Atmospheric Environment*, 101, 23-33,
27 10.1016/j.atmosenv.2014.11.012, 2015.

28 Cubison, M., Ortega, A., Hayes, P., Farmer, D., Day, D., Lechner, M., Brune, W., Apel,
29 E., Diskin, G., Fisher, J., Fuelberg, H., Hecobian, A., Knapp, D., Mikoviny, T., Riemer,

1 D., Sachse, G., Sessions, W., Weber, R., Weinheimer, A., Wisthaler, A., and Jimenez, J.:
2 Effects of aging on organic aerosol from open biomass burning smoke in aircraft and
3 laboratory studies, *Atmospheric Chemistry and Physics*, 11, 12049-12064, 10.5194/acp-
4 11-12049-2011, 2011.

5 DeCarlo, P., Kimmel, J., Trimborn, A., Northway, M., Jayne, J., Aiken, A., Gonin, M.,
6 Fuhrer, K., Horvath, T., Docherty, K., Worsnop, D., and Jimenez, J.: Field-deployable,
7 high-resolution, time-of-flight aerosol mass spectrometer, *Analytical Chemistry*, 78, 8281-
8 8289, 10.1021/ac061249n, 2006.

9 DeCarlo, P. F., Dunlea, E. J., Kimmel, J. R., Aiken, A. C., Sueper, D., Crounse, J.,
10 Wennberg, P. O., Emmons, L., Shinozuka, Y., Clarke, A., Zhou, J., Tomlinson, J., Collins,
11 D. R., Knapp, D., Weinheimer, A. J., Montzka, D. D., Campos, T., and Jimenez, J. L.: Fast
12 airborne aerosol size and chemistry measurements above Mexico City and Central Mexico
13 during the MILAGRO campaign, *Atmospheric Chemistry and Physics*, 8, 4027-4048,
14 2008.

15 Decesari, S., et al.: The 2012 PEGASOS-SUPERSITO Po Valley campaign: an overview,
16 in preparation.

17 Duplissy, J., DeCarlo, P. F., Dommen, J., Alfarra, M. R., Metzger, A., Barmpadimos, I.,
18 Prevot, A. S. H., Weingartner, E., Tritscher, T., Gysel, M., Aiken, A. C., Jimenez, J. L.,
19 Canagaratna, M. R., Worsnop, D. R., Collins, D. R., Tomlinson, J., and Baltensperger, U.:
20 Relating hygroscopicity and composition of organic aerosol particulate matter,
21 *Atmospheric Chemistry and Physics*, 11, 1155-1165, 10.5194/acp-11-1155-2011, 2011.

22 Fischer, H., Kormann, R., Klupfel, T., Gurk, C., Konigstedt, R. K., Parchatka, U., Muhle,
23 J., Rhee, T. S., Brenninkmeijer, C. A. M., Bonasoni, P., and Stohl, A.: Ozone production
24 and trace gas correlations during the June 2000 MINATROC intensive measurement
25 campaign at Mt. Cimone, *Atmospheric Chemistry and Physics*, 3, 725-738, 2003.

26 Freney, E. J., Sellegri, K., Canonaco, F., Boulon, J., Hervo, M., Weigel, R., Pichon, J. M.,
27 Colomb, A., Prevot, A. S. H., and Laj, P.: Seasonal variations in aerosol particle
28 composition at the puy-de-Dome research station in France, *Atmospheric Chemistry and*
29 *Physics*, 11, 13047-13059, 10.5194/acp-11-13047-2011, 2011.

1 Gilardoni, S., Liu, S., Takahama, S., Russell, L. M., Allan, J. D., Steinbrecher, R., Jimenez,
2 J. L., De Carlo, P. F., Dunlea, E. J., and Baumgardner, D.: Characterization of organic
3 ambient aerosol during MIRAGE 2006 on three platforms, *Atmospheric Chemistry and*
4 *Physics*, 9, 5417-5432, 2009.

5 Gilardoni, S., Massoli, P., Giulianelli, L., Rinaldi, M., Paglione, M., Pollini, F., Lanconelli,
6 C., Poluzzi, V., Carbone, S., Hillamo, R., Russell, L. M., Facchini, M. C., and Fuzzi, S.:
7 Fog scavenging of organic and inorganic aerosol in the Po Valley, *Atmospheric Chemistry*
8 *and Physics*, 14, 6967-6981, 10.5194/acp-14-6967-2014, 2014.

9 Hayes, P. L., Ortega, A. M., Cubison, M. J., Froyd, K. D., Zhao, Y., Cliff, S. S., Hu, W.
10 W., Toohey, D. W., Flynn, J. H., Lefer, B. L., Grossberg, N., Alvarez, S., Rappenglueck,
11 B., Taylor, J. W., Allan, J. D., Holloway, J. S., Gilman, J. B., Kuster, W. C., De Gouw, J.
12 A., Massoli, P., Zhang, X., Liu, J., Weber, R. J., Corrigan, A. L., Russell, L. M., Isaacman,
13 G., Worton, D. R., Kreisberg, N. M., Goldstein, A. H., Thalman, R., Waxman, E. M.,
14 Volkamer, R., Lin, Y. H., Surratt, J. D., Kleindienst, T. E., Offenberg, J. H., Dusanter, S.,
15 Griffith, S., Stevens, P. S., Brioude, J., Angevine, W. M., and Jimenez, J. L.: Organic
16 aerosol composition and sources in Pasadena, California, during the 2010 CalNex
17 campaign, *Journal of Geophysical Research-Atmospheres*, 118, 9233-9257,
18 10.1002/jgrd.50530, 2013.

19 Heald, C. L., Kroll, J. H., Jimenez, J. L., Docherty, K. S., DeCarlo, P. F., Aiken, A. C.,
20 Chen, Q., Martin, S. T., Farmer, D. K., and Artaxo, P.: A simplified description of the
21 evolution of organic aerosol composition in the atmosphere, *Geophysical Research Letters*,
22 37, 10.1029/2010gl042737, 2010.

23 Henne, S., Furger, M., and Prevot, A. S. H.: Climatology of mountain venting-induced
24 elevated moisture layers in the lee of the Alps, *Journal of Applied Meteorology*, 44, 620-
25 633, 10.1175/jam2217.1, 2005.

26 Henne, S., Klausen, J., Junkermann, W., Kariuki, J. M., Aseyo, J. O., and Buchmann, B.:
27 Representativeness and climatology of carbon monoxide and ozone at the global GAW
28 station Mt. Kenya in equatorial Africa, *Atmospheric Chemistry and Physics*, 8, 3119-3139,
29 2008.

1 Hildebrandt, L., Kostenidou, E., Mihalopoulos, N., Worsnop, D., Donahue, N., and Pandis,
2 S.: Formation of highly oxygenated organic aerosol in the atmosphere: Insights from the
3 Finokalia aerosol measurement experiments, *Geophysical Research Letters*, 37,
4 10.1029/2010gl045193, 2010.

5 Hock, N., Schneider, J., Borrmann, S., Roempp, A., Moortgat, G., Franze, T., Schauer, C.,
6 Poeschl, U., Plass-Duelmer, C., and Berresheim, H.: Rural continental aerosol properties
7 and processes observed during the Hohenpeissenberg Aerosol Characterization
8 Experiment (HAZE2002), *Atmospheric Chemistry and Physics*, 8, 603-623, 2008.

9 Holzinger, R., Goldstein, A., Hayes, P., Jimenez, J., and Timkovsky, J.: Chemical
10 evolution of organic aerosol in Los Angeles during the CalNex 2010 study, *Atmospheric*
11 *Chemistry and Physics*, 13, 10125-10141, 10.5194/acp-13-10125-2013, 2013.

12 Jayne, J., Leard, D., Zhang, X., Davidovits, P., Smith, K., Kolb, C., and Worsnop, D.:
13 Development of an aerosol mass spectrometer for size and composition analysis of
14 submicron particles, *Aerosol Science and Technology*, 33, 49-70,
15 10.1080/027868200410840, 2000.

16 Jimenez, J., Canagaratna, M., Donahue, N., Prevot, A., Zhang, Q., Kroll, J., DeCarlo, P.,
17 Allan, J., Coe, H., Ng, N., Aiken, A., Docherty, K., Ulbrich, I., Grieshop, A., Robinson,
18 A., Duplissy, J., Smith, J., Wilson, K., Lanz, V., Hueglin, C., Sun, Y., Tian, J., Laaksonen,
19 A., Raatikainen, T., Rautiainen, J., Vaattovaara, P., Ehn, M., Kulmala, M., Tomlinson, J.,
20 Collins, D., Cubison, M., Dunlea, E., Huffman, J., Onasch, T., Alfarra, M., Williams, P.,
21 Bower, K., Kondo, Y., Schneider, J., Drewnick, F., Borrmann, S., Weimer, S., Demerjian,
22 K., Salcedo, D., Cottrell, L., Griffin, R., Takami, A., Miyoshi, T., Hatakeyama, S.,
23 Shimono, A., Sun, J., Zhang, Y., Dzepina, K., Kimmel, J., Sueper, D., Jayne, J., Herndon,
24 S., Trimborn, A., Williams, L., Wood, E., Middlebrook, A., Kolb, C., Baltensperger, U.,
25 and Worsnop, D.: Evolution of organic aerosols in the atmosphere, *Science*, 326, 1525-
26 1529, 10.1126/science.1180353, 2009.

27 Jimenez, J. L., Jayne, J. T., Shi, Q., Kolb, C. E., Worsnop, D. R., Yourshaw, I., Seinfeld,
28 J. H., Flagan, R. C., Zhang, X. F., Smith, K. A., Morris, J. W., and Davidovits, P.: Ambient
29 aerosol sampling using the Aerodyne aerosol mass spectrometer, *Journal of Geophysical*
30 *Research-Atmospheres*, 108, 10.1029/2001jd001213, 2003.

1 Kroll, J., Smith, J., Che, D., Kessler, S., Worsnop, D., and Wilson, K.: Measurement of
2 fragmentation and functionalization pathways in the heterogeneous oxidation of oxidized
3 organic aerosol, *Physical Chemistry Chemical Physics*, 11, 8005-8014, 10.1039/b905289e,
4 2009.

5 Kroll, J., Donahue, N., Jimenez, J., Kessler, S., Canagaratna, M., Wilson, K., Altieri, K.,
6 Mazzoleni, L., Wozniak, A., Bluhm, H., Mysak, E., Smith, J., Kolb, C., and Worsnop, D.:
7 Carbon oxidation state as a metric for describing the chemistry of atmospheric organic
8 aerosol, *Nature Chemistry*, 3, 133-139, 10.1038/nchem.948|10.1038/NCHEM.948, 2011.

9 Lambe, A. T., Ahern, A. T., Williams, L. R., Slowik, J. G., Wong, J. P. S., Abbatt, J. P. D.,
10 Brune, W. H., Ng, N. L., Wright, J. P., Croasdale, D. R., Worsnop, D. R., Davidovits, P.,
11 and Onasch, T. B.: Characterization of aerosol photooxidation flow reactors:
12 heterogeneous oxidation, secondary organic aerosol formation and cloud condensation
13 nuclei activity measurements, *Atmospheric Measurement Techniques*, 4, 445-461,
14 10.5194/amt-4-445-2011, 2011.

15 Lanz, V., Alfarra, M., Baltensperger, U., Buchmann, B., Hueglin, C., Szidat, S., Wehrli,
16 M., Wacker, L., Weimer, S., Caseiro, A., Puxbaum, H., and Prevot, A.: Source attribution
17 of submicron organic aerosols during wintertime inversions by advanced factor analysis of
18 aerosol mass spectra, *Environmental Science & Technology*, 42, 214-220,
19 10.1021/es0707207, 2008.

20 Lanz, V. A., Prevot, A. S. H., Alfarra, M. R., Weimer, S., Mohr, C., DeCarlo, P. F., Gianini,
21 M. F. D., Hueglin, C., Schneider, J., Favez, O., D'Anna, B., George, C., and Baltensperger,
22 U.: Characterization of aerosol chemical composition with aerosol mass spectrometry in
23 Central Europe: an overview, *Atmospheric Chemistry and Physics*, 10, 10453-10471,
24 10.5194/acp-10-10453-2010, 2010.

25 Liu, P. S. K., Deng, R., Smith, K. A., Williams, L. R., Jayne, J. T., Canagaratna, M. R.,
26 Moore, K., Onasch, T. B., Worsnop, D. R., and Deshler, T.: Transmission efficiency of an
27 aerodynamic focusing lens system: Comparison of model calculations and laboratory
28 measurements for the Aerodyne Aerosol Mass Spectrometer, *Aerosol Science and*
29 *Technology*, 41, 721-733, 10.1080/02786820701422278, 2007.

1 Marengo, F., Bonasoni, P., Calzolari, F., Ceriani, M., Chiari, M., Cristofanelli, P.,
2 D'Alessandro, A., Fermo, P., Lucarelli, F., Mazzei, F., Nava, S., Piazzalunga, A., Prati, P.,
3 Valli, G., and Vecchi, R.: Characterization of atmospheric aerosols at Monte Cimone, Italy,
4 during summer 2004: Source apportionment and transport mechanisms, *Journal of*
5 *Geophysical Research-Atmospheres*, 111, 10.1029/2006jd007145, 2006.

6 Marinoni, A., Cristofanelli, P., Calzolari, F., Roccatò, F., Bonafe, U., and Bonasoni, P.:
7 Continuous measurements of aerosol physical parameters at the Mt. Cimone GAW Station
8 (2165 m asl, Italy), *Science of the Total Environment*, 391, 241-251,
9 10.1016/j.scitotenv.2007.10.004, 2008.

10 Massoli, P., Lambe, A. T., Ahern, A. T., Williams, L. R., Ehn, M., Mikkilä, J., Canagaratna,
11 M. R., Brune, W. H., Onasch, T. B., Jayne, J. T., Petaja, T., Kulmala, M., Laaksonen, A.,
12 Kolb, C. E., Davidovits, P., and Worsnop, D. R.: Relationship between aerosol oxidation
13 level and hygroscopic properties of laboratory generated secondary organic aerosol (SOA)
14 particles, *Geophysical Research Letters*, 37, 10.1029/2010gl045258, 2010.

15 Middlebrook, A. M., Bahreini, R., Jimenez, J. L., and Canagaratna, M. R.: Evaluation of
16 composition-dependent collection efficiencies for the Aerodyne aerosol mass spectrometer
17 using field data, *Aerosol Science and Technology*, 46, 258-271,
18 10.1080/02786826.2011.620041, 2012.

19 Mohr, C., DeCarlo, P., Heringa, M., Chirico, R., Slowik, J., Richter, R., Reche, C.,
20 Alastuey, A., Querol, X., Seco, R., Penuelas, J., Jimenez, J., Crippa, M., Zimmermann, R.,
21 Baltensperger, U., and Prevot, A.: Identification and quantification of organic aerosol from
22 cooking and other sources in Barcelona using aerosol mass spectrometer data, *Atmospheric*
23 *Chemistry and Physics*, 12, 1649-1665, 10.5194/acp-12-1649-2012, 2012.

24 Morgan, W., Allan, J., Bower, K., Highwood, E., Liu, D., McMeeking, G., Northway, M.,
25 Williams, P., Krejci, R., and Coe, H.: Airborne measurements of the spatial distribution of
26 aerosol chemical composition across Europe and evolution of the organic fraction,
27 *Atmospheric Chemistry and Physics*, 10, 4065-4083, 10.5194/acp-10-4065-2010, 2010.

28 Ng, N., Canagaratna, M., Zhang, Q., Jimenez, J., Tian, J., Ulbrich, I., Kroll, J., Docherty,
29 K., Chhabra, P., Bahreini, R., Murphy, S., Seinfeld, J., Hildebrandt, L., Donahue, N.,

1 DeCarlo, P., Lanz, V., Prevot, A., Dinar, E., Rudich, Y., and Worsnop, D.: Organic aerosol
2 components observed in Northern Hemispheric datasets from aerosol mass spectrometry,
3 *Atmospheric Chemistry and Physics*, 10, 4625-4641, 10.5194/acp-10-4625-2010, 2010.

4 Ng, N. L., Canagaratna, M. R., Jimenez, J. L., Chhabra, P. S., Seinfeld, J. H., and Worsnop,
5 D. R.: Changes in organic aerosol composition with aging inferred from aerosol mass
6 spectra, *Atmospheric Chemistry and Physics*, 11, 6465-6474, 10.5194/acp-11-6465-2011,
7 2011.

8 Paatero, P., and Tapper, U.: Positive matrix factorization - a nonnegative factor model with
9 optimal utilization of error-estimates of data values, *Environmetrics*, 5, 111-126,
10 10.1002/env.3170050203, 1994.

11 Pang, Y., Turpin, B. J., and Gundel, L. A.: On the importance of organic oxygen for
12 understanding organic aerosol particles, *Aerosol Science and Technology*, 40, 128-133,
13 10.1080/02786820500423790, 2006.

14 Petzold, A., Kramer, H., and Schonlinner, M.: Continuous measurement of atmospheric
15 black carbon using a multi-angle absorption photometer, *Environmental Science and*
16 *Pollution Research*, 78-82, 2002.

17 Prevot, A. S. H., Dommen, J., and Baumle, M.: Influence of road traffic on volatile organic
18 compound concentrations in and above a deep Alpine valley, *Atmospheric Environment*,
19 34, 4719-4726, 10.1016/s1352-2310(00)00254-5, 2000.

20 Putaud, J., Van Dingenen, R., Dell'Acqua, A., Raes, F., Matta, E., Decesari, S., Facchini,
21 M., and Fuzzi, S.: Size-segregated aerosol mass closure and chemical composition in
22 Monte Cimone (I) during MINATROC, *Atmospheric Chemistry and Physics*, 4, 889-902,
23 2004.

24 Saarikoski, S., Carbone, S., Decesari, S., Giulianelli, L., Angelini, F., Canagaratna, M., Ng,
25 N. L., Trimborn, A., Facchini, M. C., Fuzzi, S., Hillamo, R., and Worsnop, D.: Chemical
26 characterization of springtime submicrometer aerosol in Po Valley, Italy, *Atmospheric*
27 *Chemistry and Physics*, 12, 8401-8421, 10.5194/acp-12-8401-2012, 2012.

28 Schuepbach, E., Friedli, T. K., Zanis, P., Monks, P. S., and Penkett, S. A.: State space
29 analysis of changing seasonal ozone cycles (1988-1997) at Jungfraujoch (3580 m above

1 sea level) in Switzerland, *Journal of Geophysical Research-Atmospheres*, 106, 20413-
2 20427, 10.1029/2000jd900591, 2001.

3 Seinfeld, J. H., and Pankow, J. F.: Organic atmospheric particulate material, *Annual*
4 *Review of Physical Chemistry*, 54, 121-140,
5 10.1146/annurev.physchem.54.011002.103756, 2003.

6 Steinbacher, M., Zellweger, C., Schwarzenbach, B., Bugmann, S., Buchmann, B.,
7 Ordonez, C., Prevot, A. S. H., and Hueglin, C.: Nitrogen oxide measurements at rural sites
8 in Switzerland: Bias of conventional measurement techniques, *Journal of Geophysical*
9 *Research-Atmospheres*, 112, 10.1029/2006jd007971, 2007.

10 Sun, Y., Zhang, Q., Macdonald, A. M., Hayden, K., Li, S. M., Liggiio, J., Liu, P. S. K.,
11 Anlauf, K. G., Leaitch, W. R., Steffen, A., Cubison, M., Worsnop, D. R., van Donkelaar,
12 A., and Martin, R. V.: Size-resolved aerosol chemistry on Whistler Mountain, Canada with
13 a high-resolution aerosol mass spectrometer during INTEX-B, *Atmospheric Chemistry and*
14 *Physics*, 9, 3095-3111, 2009.

15 Sun, Y., Zhang, Q., Schwab, J., Demerjian, K., Chen, W., Bae, M., Hung, H., Hogrefe, O.,
16 Frank, B., Rattigan, O., and Lin, Y.: Characterization of the sources and processes of
17 organic and inorganic aerosols in New York city with a high-resolution time-of-flight
18 aerosol mass spectrometer, *Atmospheric Chemistry and Physics*, 11, 1581-1602,
19 10.5194/acp-11-1581-2011, 2011a.

20 Sun, Y. L., Zhang, Q., Schwab, J. J., Chen, W. N., Bae, M. S., Lin, Y. C., Hung, H. M.,
21 and Demerjian, K. L.: A case study of aerosol processing and evolution in summer in New
22 York City, *Atmospheric Chemistry and Physics*, 11, 12737-12750, 10.5194/acp-11-12737-
23 2011, 2011b.

24 Takegawa, N., Miyakawa, T., Kawamura, K., and Kondo, Y.: Contribution of selected
25 dicarboxylic and omega-oxocarboxylic acids in ambient aerosol to the m/z 44 signal of an
26 aerodyne aerosol mass spectrometer, *Aerosol Science and Technology*, 41, 418-437,
27 10.1080/02786820701203215, 2007.

1 Ulbrich, I., Canagaratna, M., Zhang, Q., Worsnop, D., and Jimenez, J.: Interpretation of
2 organic components from positive matrix factorization of aerosol mass spectrometric data,
3 *Atmospheric Chemistry and Physics*, 9, 2891-2918, 2009.

4 Van Krevelen, D. W.: Graphical-statistical method for the study of structure and reaction
5 processes of coal, *Fuel*, 24, 269-284, 1950.

6 Zhang, Q., Jimenez, J., Canagaratna, M., Allan, J., Coe, H., Ulbrich, I., Alfarra, M.,
7 Takami, A., Middlebrook, A., Sun, Y., Dzepina, K., Dunlea, E., Docherty, K., DeCarlo, P.,
8 Salcedo, D., Onasch, T., Jayne, J., Miyoshi, T., Shimojo, A., Hatakeyama, S., Takegawa,
9 N., Kondo, Y., Schneider, J., Drewnick, F., Borrmann, S., Weimer, S., Demerjian, K.,
10 Williams, P., Bower, K., Bahreini, R., Cottrell, L., Griffin, R., Rautiainen, J., Sun, J.,
11 Zhang, Y., and Worsnop, D.: Ubiquity and dominance of oxygenated species in organic
12 aerosols in anthropogenically-influenced Northern Hemisphere midlatitudes, *Geophysical*
13 *Research Letters*, 34, 10.1029/2007gl029979, 2007.

14 Zhang, Q., Jimenez, J., Canagaratna, M., Ulbrich, I., Ng, N., Worsnop, D., and Sun, Y.:
15 Understanding atmospheric organic aerosols via factor analysis of aerosol mass
16 spectrometry: a review, *Analytical and Bioanalytical Chemistry*, 401, 3045-3067,
17 10.1007/s00216-011-5355-y, 2011.

18
19

1 Table 1. Summary of AMS measurements at mountain sites published in the literature.

Reference	Site/ Season	Altitude (m asl)	Organics	Nitrate	Sulphate	Ammonium	Chloride	H:C	O:C	OM:OC
Hock et al. (2008)	Hohenpeissenberg/ spring	985	3.4 (50%)	1.3 (19%)	1.3 (19%)	0.7 (11%)	0.07 (1%)			
Sun et al. (2009)	Whistler Mountain/ spring	2182	1.05±1.03 (55%)	0.05±0.10 (3%)	0.58±0.41 (30%)	0.23±0.16 (12%)	-	1.66±0.06	0.83±0.17	2.28±0.23
Lanz et al. (2010)	Jungfraujoch/ spring	3580	0.7 (43%)	0.3 (18%)	0.4 (26%)	0.2 (13%)	<0.02 (<1%)			
Freney et al. (2011)	puy-de-Dôme/ autumn	1465	2.52 (34%)	1.14 (15%)	2.4(32%)	1.36 (18%)	0.02 (0.3%)	-	-	-
Freney et al. (2011)	puy-de-Dôme/ winter	1465	1.24 (23%)	1.71 (32%)	1.28 (24%)	1.08 (20%)	0.07 (1%)	-	-	-
Freney et al. (2011)	puy-de-Dôme/ summer	1465	15.59 (57%)	2.33 (9%)	5.45 (20%)	3.69 (14%)	0.06 (0.2%)	-	-	-
This study	Mt. Cimone/ summer	2165	2.8±2.4 (63%)	0.33±0.46 (7%)	0.92±0.60 (20%)	0.41±0.33 (9%)	(<1%)	1.45±0.11	0.71±0.08	2.08±0.10

2

3 Table 2. Pearson correlation coefficients (R) between the time series of the three PMF
4 factors and several gas-phase and particle tracers measured at Mt. Cimone.

	BC	CO	T	P	RH	WS	UVB	O ₃	NO _x	nitrate	sulphate	Ammonium
OOAa	0.54	0.71	0.48	0.42	0.22	-0.23	0.12	0.45	0.70	0.55	0.48	0.57
OOAb	0.35	0.27	0.36	0.25	-0.01	0.02	0.09	0.28	0.18	0.09	0.64	0.43
OOAc	0.41	0.24	0.16	0.26	-0.12	0.12	-0.10	0.58	0.02	0.12	0.49	0.38

5

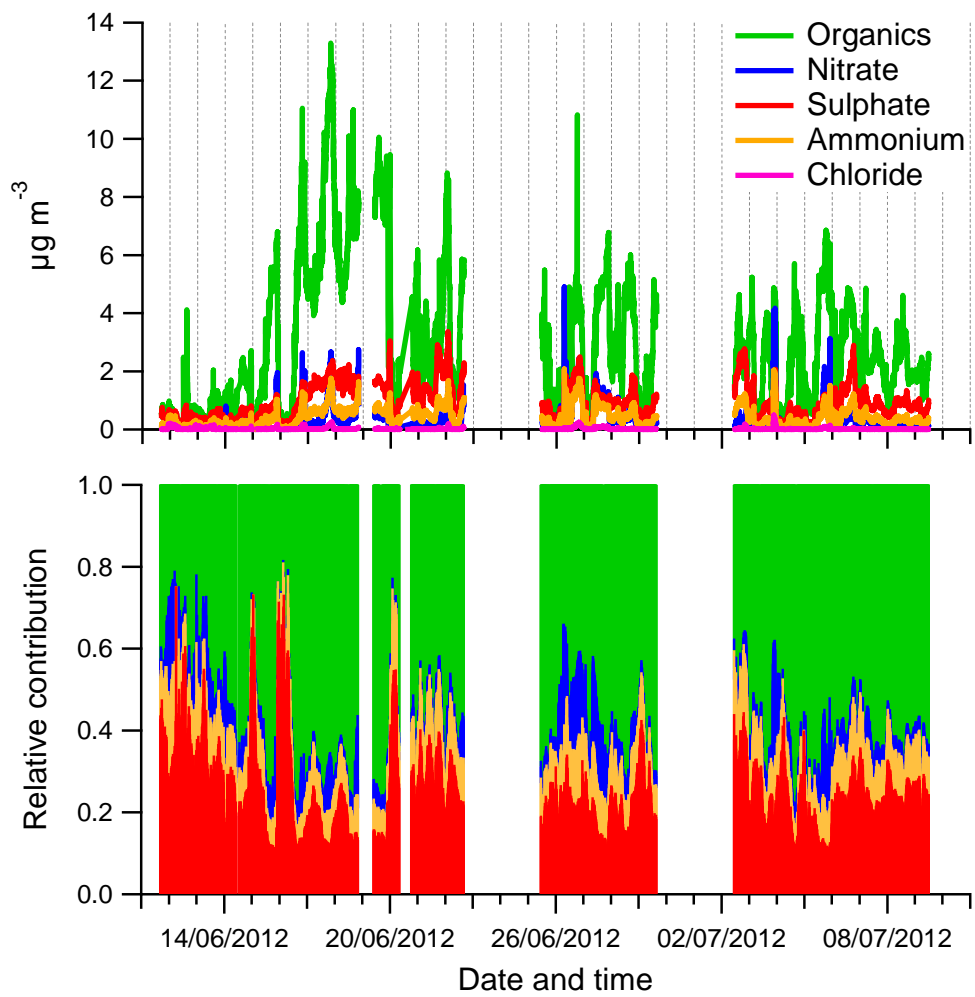
6 Table 3. Pearson correlation coefficients (R) between the profiles of the three PMF factors
7 and reference high resolution factor profiles found in the literature.

	Saarikoski et al., 2012						Mohr et al., 2012				Crippa et al., 2013		
	OOAa	OOAb	OOAc	HOA	BBOA	NOA	BBOA	HOA	LVOA	SVOA	SVOOA	LVOOA	HOA
OOAa	0.93	0.92	0.90	0.75	0.38	0.40	0.62	0.19	0.87	0.81	0.86	0.93	0.50
OOAb	0.94	0.92	0.90	0.70	0.30	0.34	0.61	0.17	0.91	0.81	0.81	0.93	0.45
OOAc	0.97	0.94	0.97	0.58	0.21	0.10	0.31	0.07	0.95	0.76	0.59	0.94	0.32

8

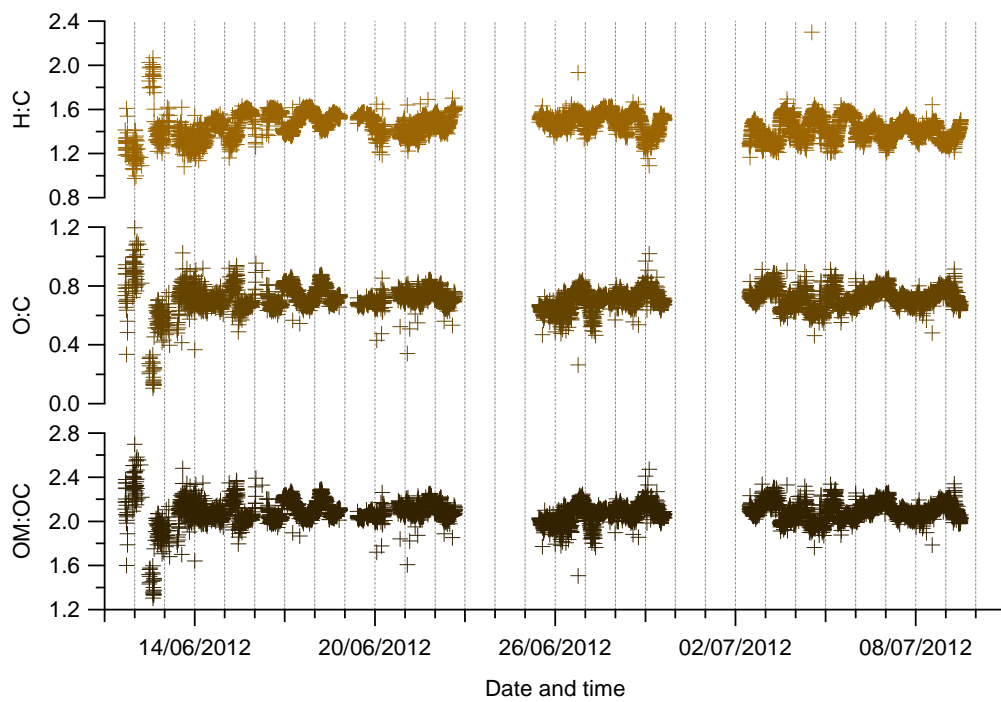
9

10



1
2
3
4
5
6

Figure 1. Time series and relative contribution of the main NR-PM₁ components. Time is local (UTC+2 hr).

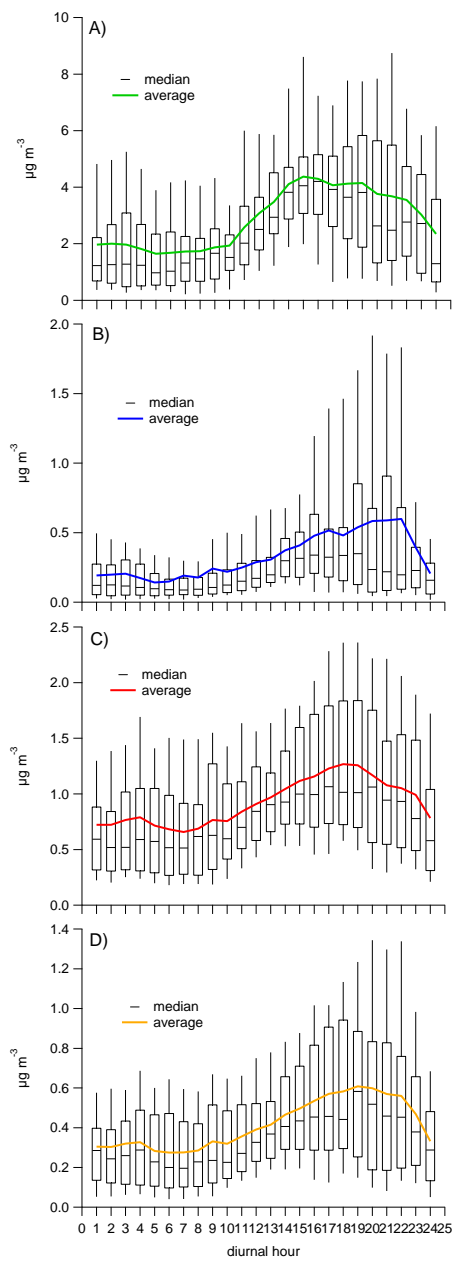


1

2

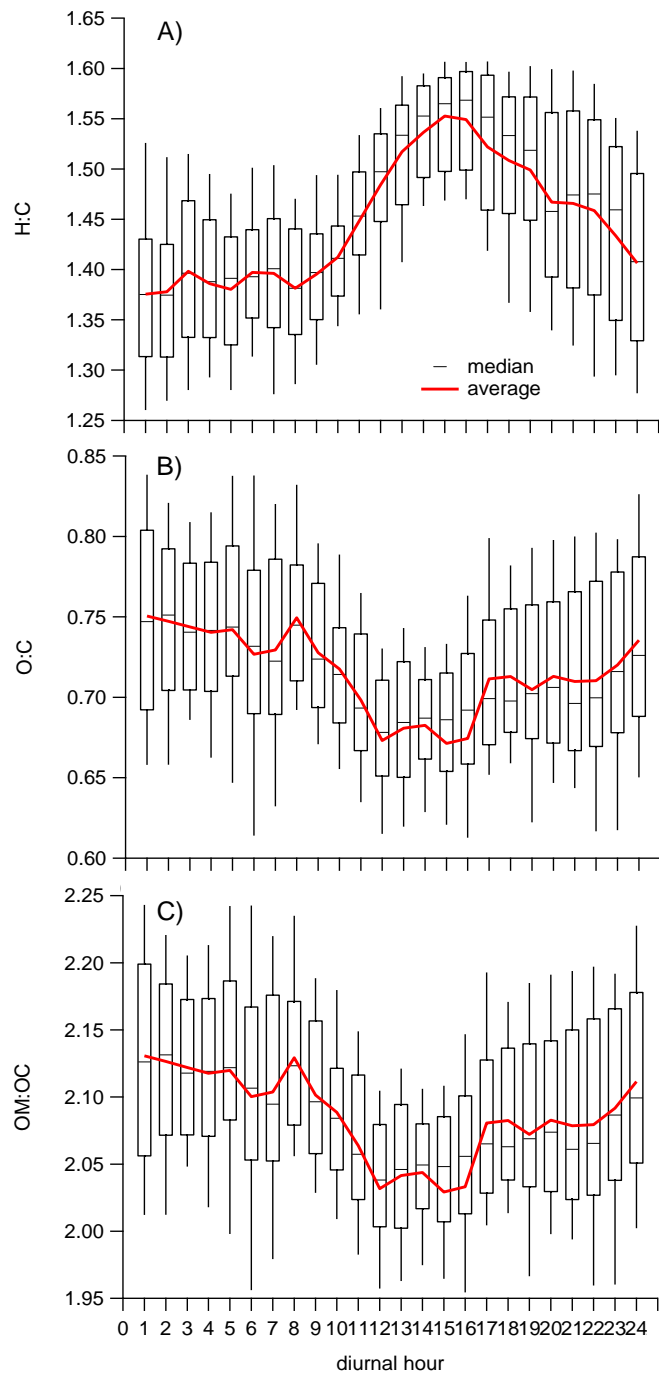
3 Figure 2. Time series of the H:C, O:C and OM:OC ratios. Time is local (UTC+2 hr).

4



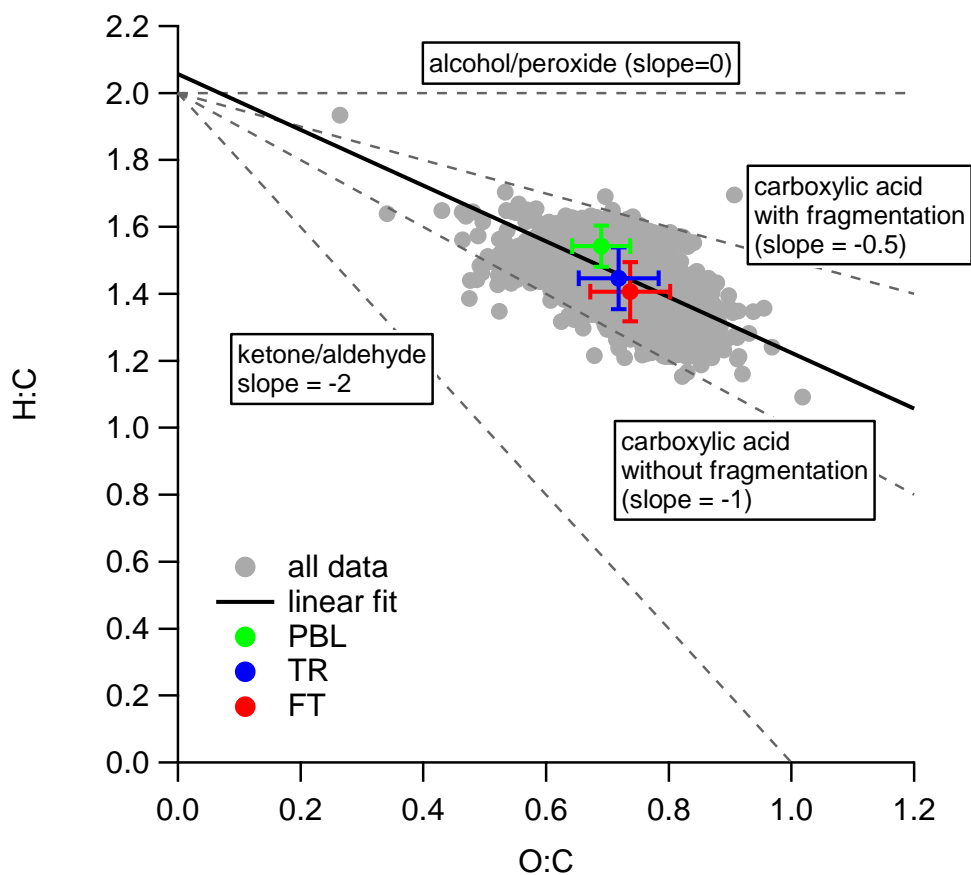
1
2
3
4
5
6

Figure 3. Daily trends of (A) organics, (B) nitrate, (C) sulphate and (D) ammonium. Boxes represent median, 25th and 75th percentile; whiskers indicates 10th and 90th percentile. Time is local (UTC+2 hr).



1
2
3
4
5
6

Figure 4. Daily trends of the (A) H:C, (B) O:C and (C) OM:OC ratios. Boxes represent median, 25th and 75th percentile; whiskers indicates 10th and 90th percentile. Time is local (UTC+2 hr).

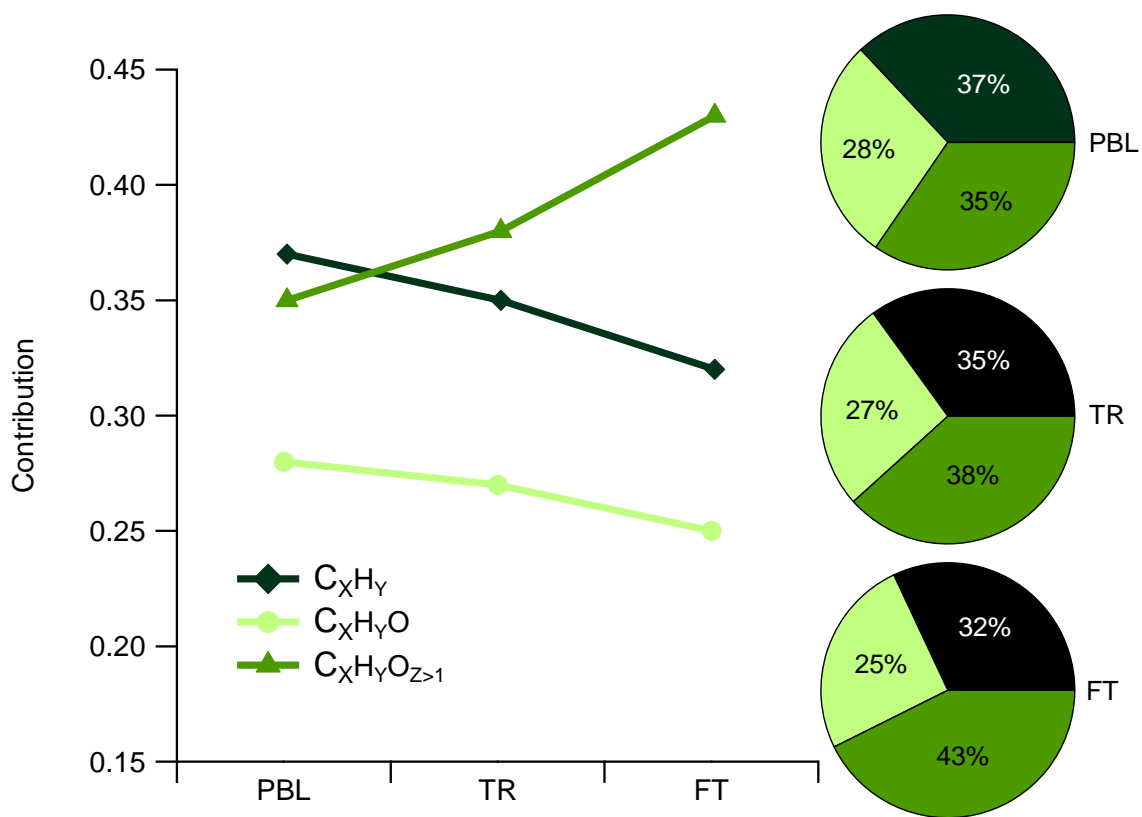


1

2

3 Figure 5. Van Krevelen diagram presenting the H:C and O:C ratios of all the data points
 4 collected during the campaign, superimposed to average values for PBL, TR and FT
 5 samples. The solid line represents the fit to the data (not constrained to H:C=2). Dashed
 6 lines describes oxidation reactions occurring through addition of carbonyl groups (slope =
 7 -2 (Heald et al., 2010)), carboxylic acid without fragmentation (slope = -1 (Heald et al.,
 8 2010)), carboxylic acid with fragmentation (slope = -0.5 (Ng et al., 2011)) and
 9 alcohol/peroxide (slope = 0 (Heald et al., 2010)).

10

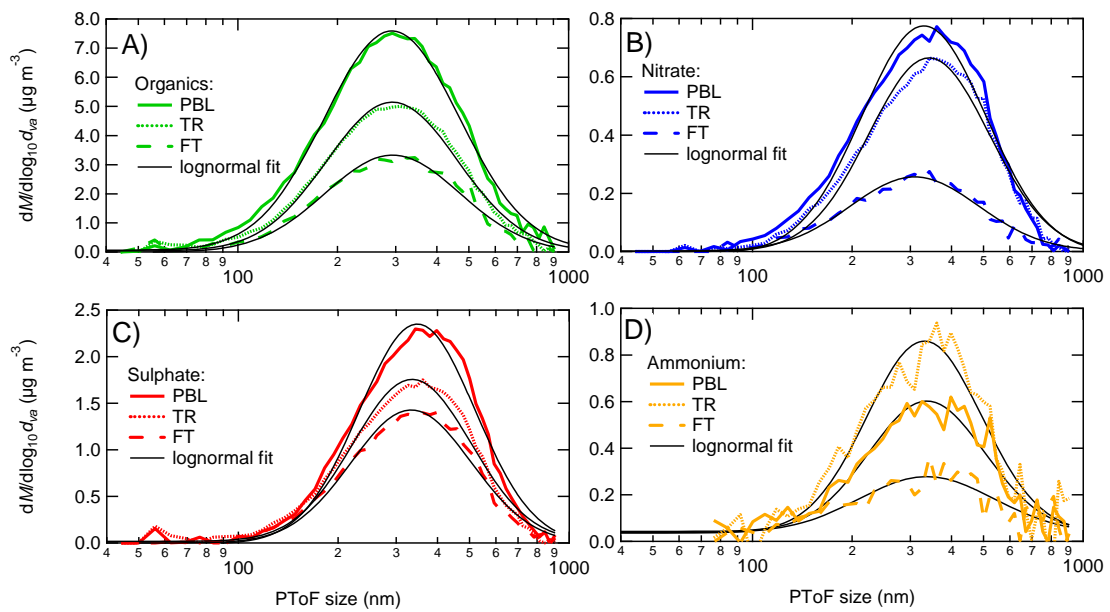


1

2

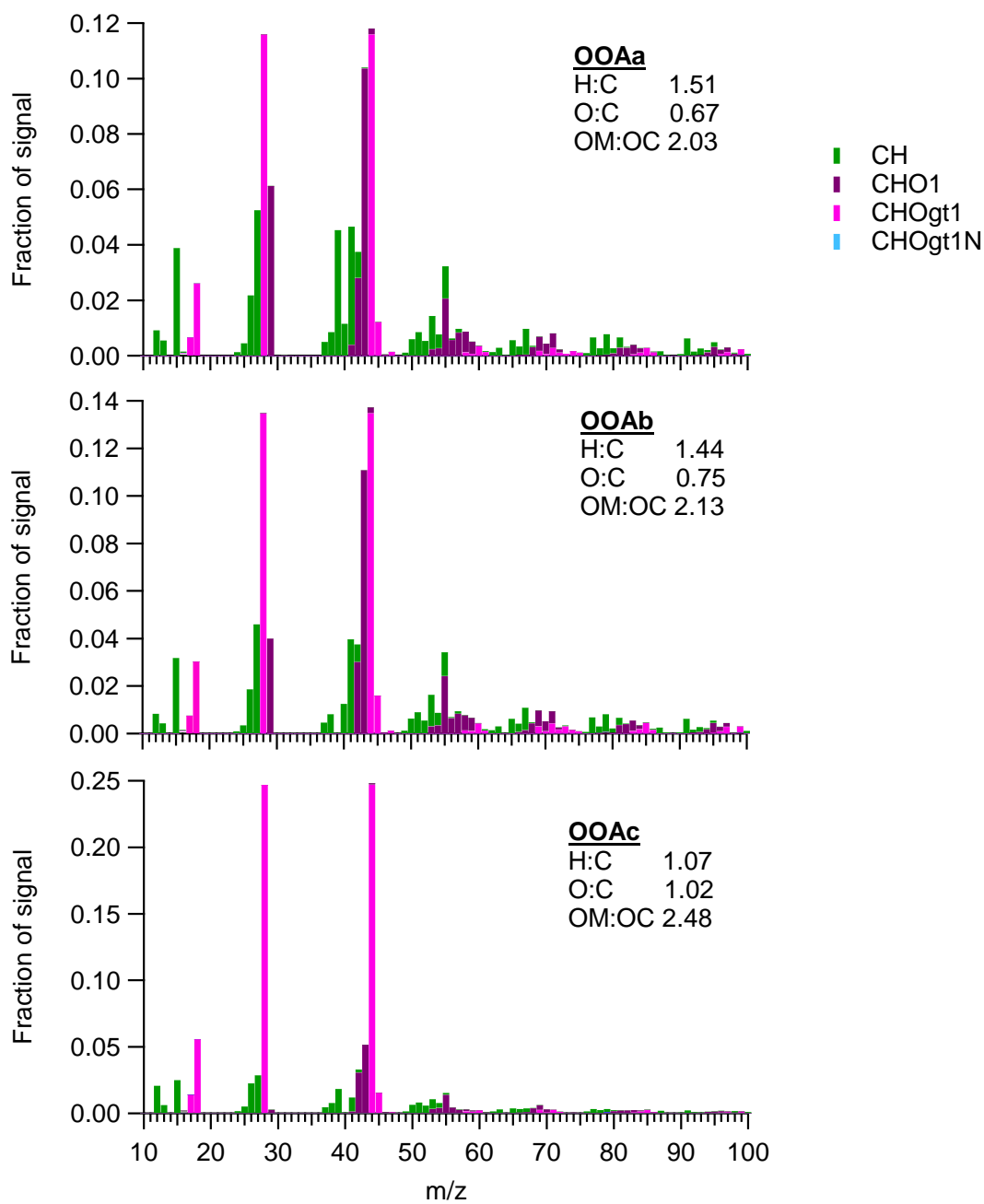
3 Figure 6. Contribution of organic fragments containing only carbon and hydrogen (C_xH_y),
 4 organic fragments containing carbon, hydrogen and one oxygen atom ($C_xH_yO_1$) and
 5 organic fragments containing carbon, hydrogen and more than one oxygen atom
 6 ($C_xH_yO_{z>1}$) in PBL, TR and FT samples.

7



1
2
3
4
5

Figure 7. Size distribution of (A) organics, (B) nitrate, (C) sulphate and (D) ammonium in PBL, TR and FT samples. Lognormal fits are reported as black lines.

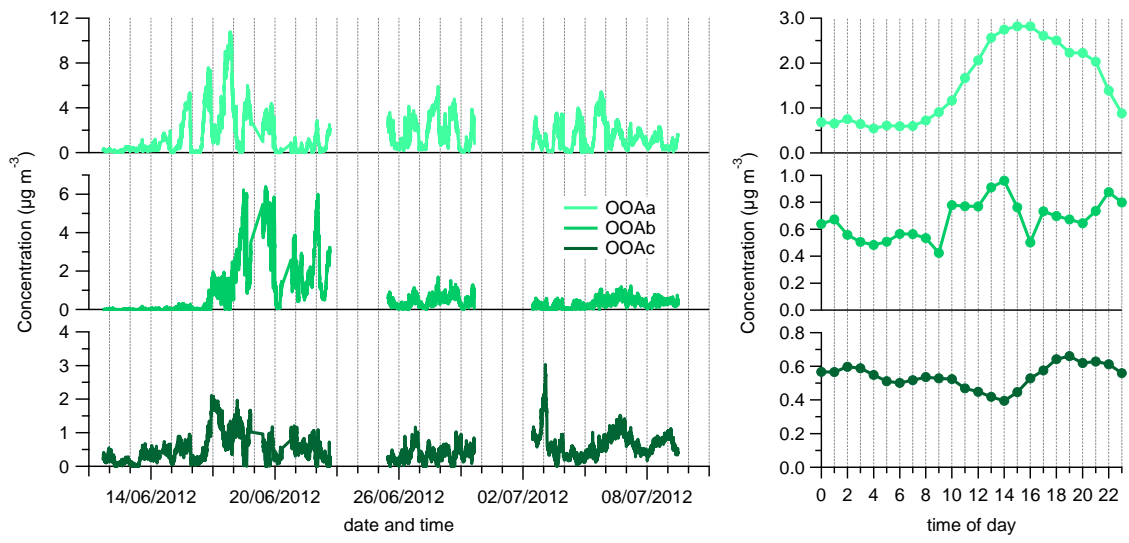


1

2

3 Figure 8. High resolution mass spectra of the three factors extracted by PMF. Insets in each
4 plot reports the results of the elemental analysis (from the I-A method).

5

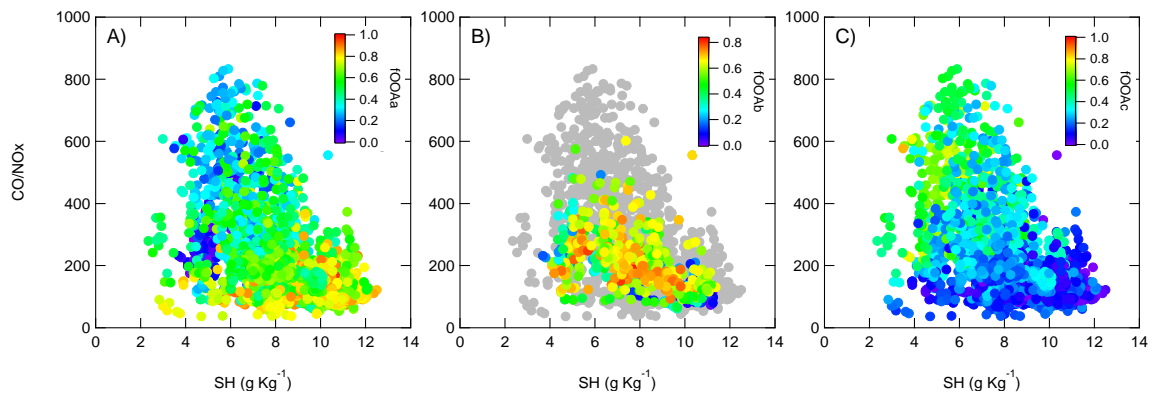


1

2

3 Figure 9. Time series and diurnal trend of the three factors extracted by PMF.

4



1

2

3 Figure 10. CO/NO_x ratio vs. SH, colour coded by the contribution of factors (A) OOAa,
 4 (B) OOAb and (C) OOAc. In (B) only the data points corresponding to OOAb maximum
 5 contribution period (17-23 June) have been coloured, to make the plot clearer.

6

7